Available online at www.sciencedirect.com

SCIENCE DIRECT

ELSEVIER

Genomics 87 (2006) 665–672

GENOMICS

www.elsevier.com/locate/ygeno

Method

Functional screening for proapoptotic genes by reverse transfection cell array technology

Otto Mannherz, Daniel Mertens, Meinhard Hahn, Peter Lichter *

Division of Molecular Genetics (B060), Deutsches Krebsforschungszentrum, Im Neuenheimer Feld 280, D-69120 Heidelberg, Germany

Received 30 September 2005; accepted 19 December 2005
Available online 28 February 2006

Abstract

Application of mathematical algorithms to sequenced whole genomes revealed a large number of predicted genes, requiring functional assays for their characterization in a high-throughput manner. Here, we report on the development of a screening assay, which is based on reverse transfection of cellular arrays and subsequent analysis of cell morphology to identify novel proapoptotic genes. Expression plasmids containing full-length cDNAs were cotransfected with the reporter plasmid *pEYFP* to screen for apoptotic body formation, based on EYFP fluorescence. The assay was validated and applied to 382 human sequence-verified full-length open reading frames, most of them of unknown function. In this initial screening, proapoptotic effects could be demonstrated for 10 of these genes. For 6 of them apoptosis induction could be confirmed both by TUNEL assay and by FACS analysis of cells stained according to Nicoletti: 1 gene was not yet annotated for an apoptotic function (*ST6GAL2*), while 5 genes were without annotated function (*FLJ20551, CXorf12, FAM105A, TMEM66, C19orf4*). Our study demonstrates the potential of this method to characterize functionally genes of unknown function in a highly parallel format.

Keywords: Reverse transfection; Cell array technology; Apoptosis; Caspase; Nuclear morphology

Analysis of sequenced genomes disclosed a plethora of genes of unknown function, providing opportunities for genome-wide functional characterizations [1]. Methods used to characterize genes of unknown function include (i) algorithms searching for homologies between protein subdomains [2,3], (ii) overexpression of the gene of question, and (iii) knockout or knockdown of individual genes [4]. A promising technology developed for the characterization of unknown genes in a highly parallel format is the reverse transfection of arrayed cDNAs [5]. In comparison to conventional transfection, components are applied in a parallel format in a different order. First, the expression plasmid, containing the cDNA to be analyzed, is complexed with transfection reagent. The complex is subsequently spotted on a glass slide, which is overlaid in the next step with a suspension of adherently growing cells. Seeded cells will adhere to the surface, become transfected, and express the respective proteins. Following the first publication of the reverse transfection assay, the technique was applied for the development of a variety of screening assays [6–9].

To screen for apoptosis-related genes, the original protocol was adopted and modified to meet the special requirements for screening for proapoptotic genes. Assays measuring caspase activity using fluorogenic substrates or phosphatidylserine exposition by annexin V staining are limited to the detection of specific pathways only. To overcome this handicap, we assessed a late event of apoptosis, the apoptotic body formation. The main advantage of the reverse transfection technology is its potential to screen large numbers of genes for a particular function. In addition, the method allows for the assessment of not only the apoptotic phenotype but also other phenotypic changes. Furthermore, cell-based assays employing immunohistochemistry or detection of protein interaction can be easily adapted.

We proved the applicability of the assay by screening 382 randomly selected human sequence-verified, full-length ORFs for novel proapoptotic genes.

Abbreviations: ORF, open reading frame; EYFP, enhanced yellow fluorescent protein; GDM, gelatin–DNA method; LDM, lipid–DNA method; FACS, fluorescence-activated cell sorting; RZPD, Resource Center Primary Database; DAPI, 4′,6-diamidino-2-phenylindole; HEK, human embryonal kidney; TUNEL, terminal deoxynucleotidyl transferase biotin–dUTP nick-end labeling; GOA, Gene Ontology Annotation.

* Corresponding author. Fax: +49 6221 42 4639.
E-mail address: m.macleod@dkfz.de (P. Lichter).

0888-7543/$ - see front matter © 2006 Elsevier Inc. All rights reserved.
doi:10.1016/j.ygeno.2005.12.009

Results

Optimization of reverse transfection

An optimized protocol for reverse transfection was developed, based on the lipid–DNA method (LDM) [5]. In addition to the LDM, we also tested the gelatin–DNA method (GDM) [5]. For the GDM, expression plasmids were mixed with a gelatin solution and arrayed onto poly-L-lysine-coated slides. The arrays were subsequently incubated with the transfection reagent. For transfection via the LDM, expression plasmids were premixed with the transfection reagent and the gelatin solution and printed onto the slides. After either of the two methods, the arrays were overlaid with a suspension of adherently growing cells. Two days after transfection, the cells were fixed and analyzed.

We tested both methods for suitability for reverse transfection, using the *pEYFP* plasmid as a reporter for transfection efficiency. The LDM yielded consistently good expression results over the whole spotted surface. In our hands, using the GDM, often large areas were not transfected and many spots did not show detectable EYFP fluorescence. Due to the homogeneous transfection of the array obtained with the LDM, we decided to use it as the basis for our screening assay.

Regarding the LDM, the concentrations of sucrose and gelatin in the transfection mixture play an important role in both transfection efficiency and spot integrity. Low sucrose concentration is insufficient to maintain the DNA–transfection reagent complex stable, whereas high sucrose concentration disturbs immobilization, as transfected cells are spread outside the spots (Fig. 1A). Low gelatin concentration reduces transfection efficiency (Fig. 1A). For all further experiments, we used 34 mM sucrose and 0.2% gelatin.

The transfection efficiency for HEK293T cells obtained by the optimized LDM was around 50%. To yield statistically reliable results and allow for the identification of genes with low efficacy in inducing apoptosis, a sufficiently high number of cells was needed. Therefore, we employed spotting pins with a delivery volume of 12.5 nl to obtain a mean spot diameter of 600 μm, which resulted in 100–400 transfected cells growing within these spots.

Detection of apoptosis after reverse transfection

Our goal was to test for a late apoptotic marker, covering various apoptotic pathways. After reverse transfection, we screened for three well-characterized events occurring at the end of the apoptotic cascade: apoptotic body formation, DNA cleavage, and fragmentation of the nucleus. As a reference gene for apoptosis induction, the proapoptotic *Bax* gene, which encodes a murine mitochondrial membrane protein, was used. To visualize apoptotic bodies, we cotransfected *pEYFP* as reporter plasmid. DNA cleavage was detected using the TUNEL assay on the cell array, which labels free 3′-OH termini with modified nucleotides in an enzymatic reaction. Fragmented nuclei were visualized by DAPI staining. Cells expressing EYFP and mouse Bax were examined for appearance of apoptotic bodies, DNA cleavage, and fragmentation of the nuclei (Fig. 1B, middle and bottom). Apoptotic bodies appeared as small intense green fluorescent blebs, accumulating EYFP. There were many more fragmented nuclei than nuclei containing cleaved DNA. Visual inspection of numerous spots revealed in each case only very few TUNEL-positive nuclei. One example is shown in Fig. 1B (see also Discussion). In addition, there were more apoptotic bodies visible than fragmented nuclei, since a single cell releases several apoptotic bodies.

Determination of gene expression levels for detection of apoptosis

The optimal range of *Bax* and reporter plasmid *pEYFP* expression had to be established to obtain optimal induction of apoptosis along with sufficient visibility of the spots and apoptotic bodies. We tested the range of *Bax* and *pEYFP* expression using 0.2–0.8 μg transfected DNA (Fig. 1B, top). The optimal ratio of *Bax/pEYFP* in the transfection mix was 1:1, using 0.6 μg of each plasmid. This ratio was used in all further screening experiments.

As a negative control, the reporter plasmid *pEYFP* was selected. *pEYFP* (0.6 μg) was printed and reversely transfected. Spots expressing the *pEYFP* plasmid alone yielded intense fluorescence due to strong expression of the EYFP protein (Fig. 1C). As a positive control, 0.6 μg of the expression vector containing *Bax* was transfected, along with 0.6 μg of *pEYFP*. Cells exhibited formation of apoptotic bodies and fragmentation of the nucleus (Fig. 1D).

Functional analysis of 382 genes of mostly unknown function

To screen for new proapoptotic proteins, 382 full-length ORFs, 92% of which were genes without annotation for a biological process, were randomly selected from Library 970 of the RZPD. We selected this library since it contains a large number of genes with unknown function. Expression plasmids

Fig. 1. Development of a screening assay for proapoptotic genes by reverse transfection. (A) Influence of sucrose and gelatin concentration on transfection efficiency and adhesion of expression plasmids. (B) Assessment of gene expression levels for detection of apoptosis. Different amounts of EYFP and a murine Bax-expressing plasmid were reversely transfected. The cells were fixed and the spots examined for appearance of apoptotic bodies. Nuclei were stained with DAPI and the TUNEL assay was performed to compare nuclear fragmentation, DNA cleavage, and appearance of apoptotic bodies. Top: Fluorescence scan of EYFP. Middle: Fluorescence image of a single spot. Bottom: Fluorescence images of the same section of a single spot. Arrows show fragmented nuclei. (C, D) Validation of the control plasmids. (C) As negative control, 0.6 μg reporter plasmid *pEYFP* was reversely transfected alone. Top left: Fluorescence scan of EYFP-expressing cell clusters with a microarray scanner. Bar, 600 μm. Top right: Fluorescence image of a single spot. Bottom left and right: Fluorescence images of DAPI-stained nuclei and EYFP-positive cells of a section of a spot. Bar, 50 μm. (D) As positive control, 0.6 μg reporter plasmid *pEYFP* and 0.6 μg expression vector containing the *Bax* gene were cotransfected. Images as in (C). (E) ST6GAL2- and EYFP-expressing cells exhibit apoptotic bodies (arrows) and fragmented nuclei (DAPI).

were cospotted in four replicates with the reporter *pEYFP* and transfected into HEK293T cells using the LDM. After fixation, the appearance of apoptotic bodies was assessed by visual inspection. As an example, *ST6GAL2* is shown in Fig. 1E. Phenotypic changes were scored only when present on at least two of the four replicate spots and on at least two of three analyzed slides. Ninety-three percent of the 382 screened ORFs displayed a normal phenotype (Table 1). Ten genes were identified, the transfection of which resulted in the appearance of apoptotic bodies. Only 1 of these, *ANT1*, was

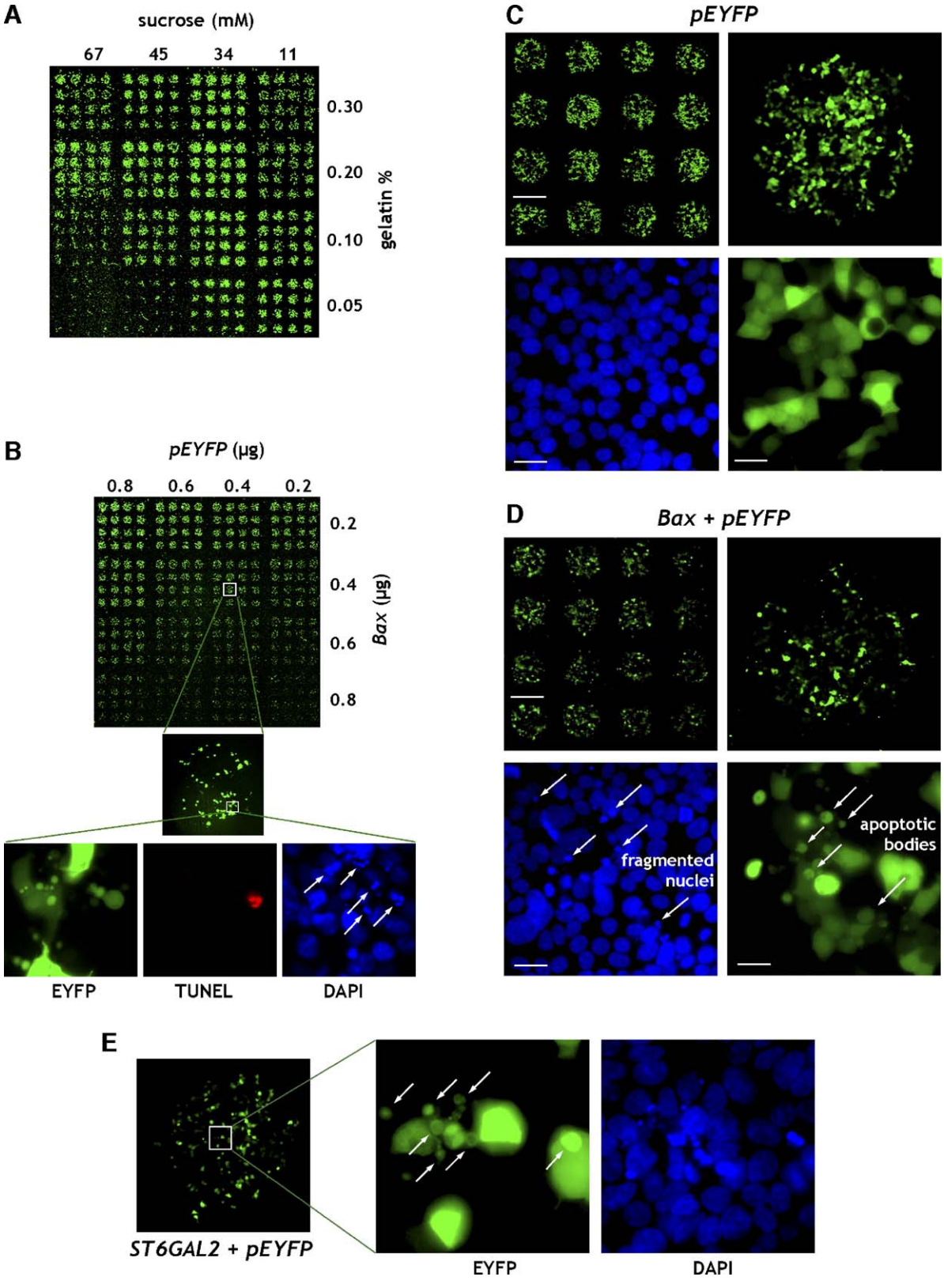

Table 1
Distribution of the observed morphological changes

Screened genes in total	382	100%
Genes causing phenotypic changes	26	6.8%
Proapoptotic genes [a]	7	1.8%
Genes causing rounded phenotype [a]	21	5.5%
Genes causing dented nuclei [a]	8	2.1%
Other morphology [a]	9	2.4%
No phenotypic changes observed	356	93.2%

[a] Overlap of phenotypes, see Table 2.

previously known to induce apoptosis [10]. The remaining 9 genes were retested for DNA cleavage by TUNEL staining without *pEYFP*. In addition to apoptotic body formation, DNA fragmentation was observed for 6 of the genes; 4 of them are shown in Fig. 2. For 1 of these, an apoptotic function had not been assigned yet (*ST6GAL2*), while 5 of the proapoptotic genes had no previously annotated function (genes *FLJ20551, CXorf12, FAM105A, TMEM66, C19orf4*). In addition to the 7 genes inducing apoptosis, 19 genes caused distinct morphological changes: rounded cells, dented nuclei, small round condensed nuclei, large nucleoli, condensed chromosome clusters, protruding cellular processes, or abnormally shaped cells (see Table 2 and Supplementary Fig. S1). Notably, overexpression of several genes causing distinct phenotypes also led to a roundish cell shape, indicating a decreased adherence to the glass slide surface (see Table 2 and Supplementary Fig. S1).

Quantitation of induction of apoptosis by the identified genes

To assess the potential for induction of apoptosis, the six validated proapoptotic genes, as well as *Bax* and the empty vector as controls, were transfected into HEK293T cells. These were subsequently subjected to Nicoletti staining after an incubation of 48 h. In this assay, the cytoplasm is removed and fragmented DNA diffuses out of the nucleus. Apoptotic nuclei can be detected based on reduced DNA content compared to the normal G1 population. After transfection, apoptotic nuclei could be measured with fluorescence-activated cell sorting

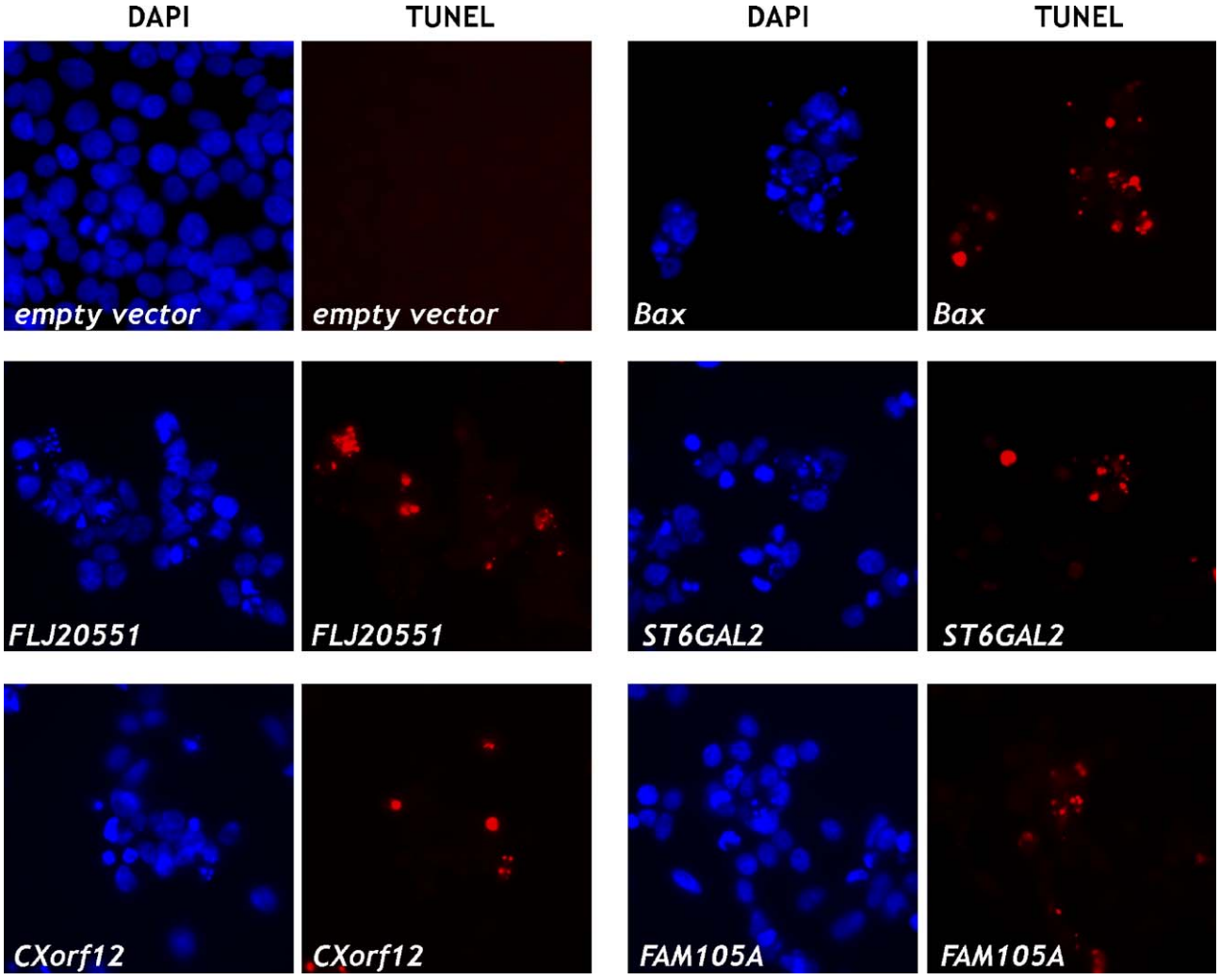

Fig. 2. Validation of the identified genes using TUNEL staining. Empty vector, *Bax*, and four of the identified proapoptotic genes were transfected into HEK293T cells. Nuclei were stained by DAPI, apoptotic nuclei were stained using the TUNEL assay.

Table 2
Phenotypic changes detected after overexpression

Gene name	Gene symbol	Accession No.	Observed phenotypes			
			Apoptosis	Rounded cells	Dented nuclei	Other morphology
Solute carrier family 25, member 4	*SLC25A4*	BC008664	+	+		
Hypothetical protein FLJ20551	*FLJ20551*	BC013194	+			
ST6 beta-galactosamide alpha-2,6-sialytranferase 2	*ST6GAL2*	BC008680	+	+		
Chromosome X open reading frame 12	*CXorf12*	BC008203	+	+	+	
Family with sequence similarity 105, member A	*FAM105A*	BC011524	+	+		
Chromosome 19 open reading frame 4	*C19orf4*	BC010446	+	+		
Transmembrane protein 66	*TMEM66*	BC015012	+	+		
Chromosome 19 open reading frame 32	*C19orf32*	BC008201		+	+	Small round condensed nuclei
Transmembrane protein 109	*TMEM109*	BC001309		+		Small round condensed nuclei
Chromosome 12 open reading frame 23	*C12orf23*	BC020522		+		Small round condensed nuclei
Chromosome 20 open reading frame 195	*C20orf195*	BC000912		+		
SFT2 domain containing 3	*SFT2D3*	BC006808		+		
Adiponectin receptor 1	*ADIPOR1*	BC010743		+		
Chromosome 14 open reading frame 169	*C14orf169*	BC011350		+		Large nucleoli
Solute carrier family 41, member 3	*SLC41A3*	BC009039		+	+	
Ring finger protein 121	*RNF121*	BC009672		+	+	
Chromosome 22 open reading frame 5	*C22orf5*	BC015489		+	+	
Transmembrane BAX inhibitor motif containing 1	*TMBIM1*	BC013428		+	+	
Transmembrane protein 112	*TMEM112*	BC010738		+	+	
Leucine-rich repeat neuronal 6A	*LRRN6A*	BC011057		+	+	
Dehydrogenase/reductase (SDR family) member 7B	*DHRS7B*	BC009679		+		
Chromosome 1 open reading frame 96	*C1orf96*	BC015419		+		Condensed chromosomes
Chromosome 16 open reading frame 56	*C16orf56*	BC015202				Condensed chromosomes
Protein phosphatase 1A (formerly 2C), magnesium-dependent, alpha isoform	*PPM1A*	BC026691				Condensed chromosomes
Transmembrane protein 24	*TMEM24*	BC022219				Neuron-like cells
Tubulin-specific chaperone cofactor e	*TBCE*	BC008654				Abnormally shaped cells

(FACS) (Fig. 3A). Two of the proapoptotic genes induced apoptosis in 30–40% of the cells (*FLJ20551, ST6GAL2*), two in 20–25% of the cells (*CXorf12, FAM105A*), and two in 7% (*C19orf4, TMEM66*) (Fig. 3B). To investigate the involvement of caspases in apoptosis execution of these genes, the pan-caspase inhibitor Z-VAD-fmk was added to each transfection setup in a parallel experiment. Apoptosis induction could be reduced to 2.5–5% by the presence of Z-VAD-fmk for the genes *FLJ20551, ST6GAL2, CXorf12, C19orf4*, and *TMEM66*. In contrast, around 10% of *Bax*- or *FAM105A*-transfected cells were driven into apoptosis.

Discussion

Optimization of reverse transfection for screening for proapoptotic genes

The reverse transfection technology allows highly parallel functional characterization of genes. It has been applied in various screening settings, including (i) a high-throughput phenotype screening microscopy platform [8], (ii) a setup for the screening of phenotypes caused by gene silencing [9], (iii) high-throughput selection of effective RNAi probes [6], and (iv) monitoring of mitogen-activated protein kinase signaling [7]. However, none of these methods has been validated in follow-up screening studies. In this work, we demonstrate that our approach based on the reverse transfection method is a powerful tool to screen for proapoptotic genes. We opted for the reverse transfection because it offers the possibility of assessing morphological changes, such as apoptotic body formation, at a high resolution. As imaging platforms for acquisition of high-resolution images of large areas become more sophisticated, application of pattern recognition software could be implemented for automated detection of apoptotic bodies.

We preferred to use the lipid–DNA transfection method, which resulted in homogeneous transfection of a given cell array. Using the GDM, the critical step was to remove the Hybri-Well chamber after incubation of the spotted array with the transfection reagent. Thereby, the chamber came into contact with parts of the arrayed surface, resulting in low transfection efficiency for large areas of the array.

For detection of apoptosis nuclear fragmentation, DNA cleavage and appearance of apoptotic bodies were compared. TUNEL staining labeled only a few of the fragmented nuclei (Fig. 1B). The TUNEL assay seems specific for a very late phase of apoptosis, which is not reached yet in the remaining fragmented nuclei. The difference between the numbers of nuclei fragmented and the TUNEL-positive nuclei (which are only a small subset of the same nuclei) is explained well by the fact that fragmentation of the DNA, detected by the TUNEL assay, takes place at a time point later than fragmentation of the nucleus [11]. Intensity and number of TUNEL-positive nuclei were not sufficient to identify apoptotic spots. In contrast, screening for apoptotic bodies showed reliable results, since apoptotic cells fragment into many apoptotic bodies. The optimal ratio of the concentration of *pEYFP* to the concentration of the expression

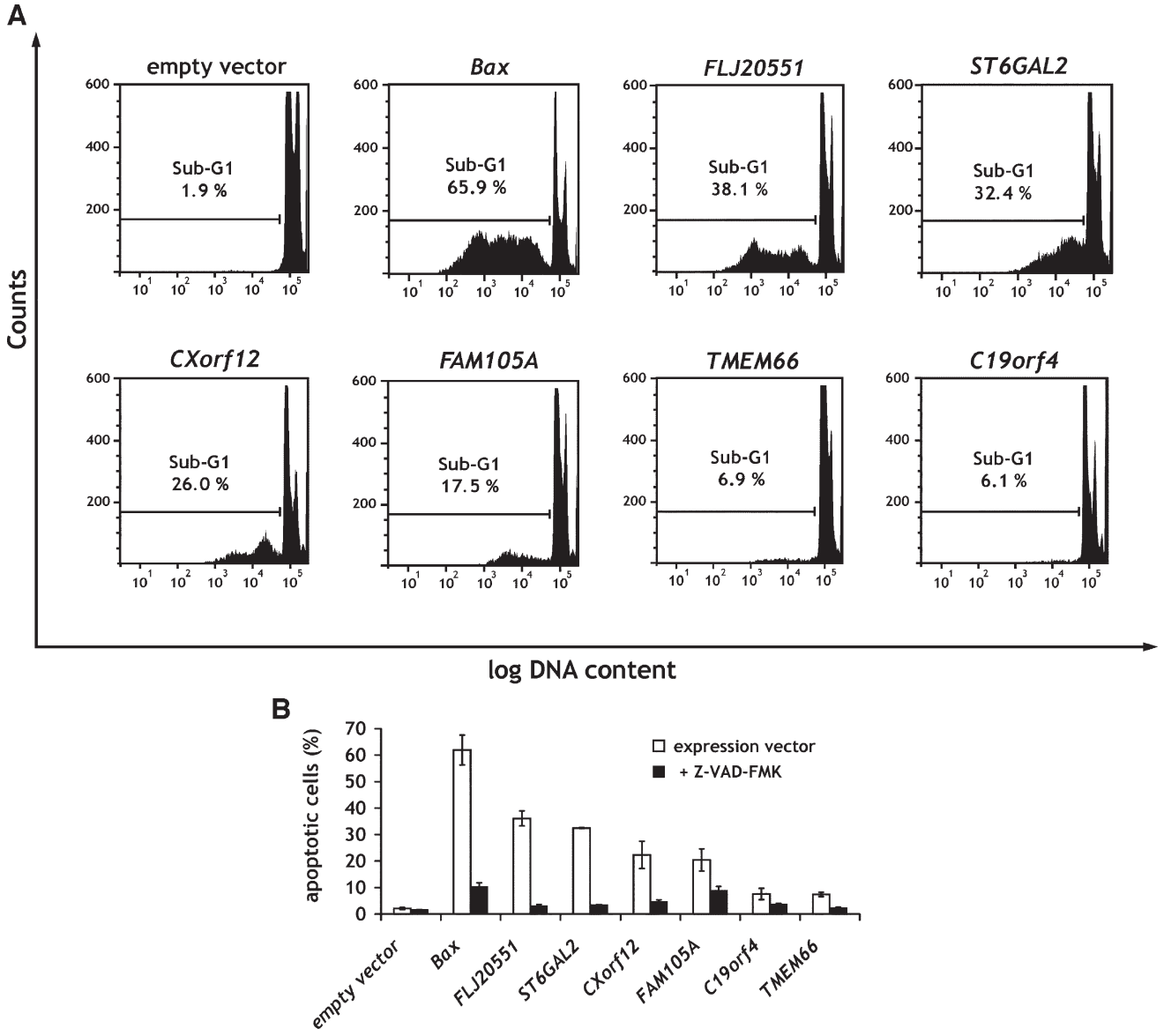

Fig. 3. Quantification of apoptotic cell populations after overexpression of the identified genes by FACS. Empty vector, *Bax*, and the identified proapoptotic genes were transfected into HEK293T cells. Harvested cells were incubated with Nicoletti buffer. Apoptotic nuclei appearing in the sub-G1 phase were quantified. (A) Histograms showing apoptotic, G1, and G2 cell populations. (B) Apoptotic cell populations were quantified from two transfection experiments, in the presence or absence of the pan-caspase inhibitor Z-VAD-fmk. Nuclei were stained using the Nicoletti buffer to quantify apoptotic cells by FACS. Error bars represent the standard deviation of two independent experiments.

clones was 1:1, using 0.6 μg of each plasmid (Fig. 1B). When replica spots of four are used for each cDNA, up to 200 different ORFs can be screened on one poly-L-lysine coated slide.

Identification of proapoptotic genes by reverse transfection of an expression library

Traditional approaches to screen for proapoptotic genes target different downstream caspases. However, detection of single caspases depicts only a subset of proapoptotic molecules. As apoptotic bodies represent an endpoint of virtually all apoptotic pathways, they are superior as phenotypic markers of apoptosis for a screening approach. Furthermore, the assay is highly specific, since the appearance of apoptotic bodies is exclusively assigned to apoptotic processes. High sensitivity of the assay could be confirmed by the quantification of apoptotic cell populations by FACS analysis: two apoptotic genes were identified by reverse transfection that induced apoptosis in only 7% of the cells as measured by FACS (*C19orf4, TMEM66*) (Fig. 3B).

THREE hundred eighty-two genes were screened, 352 of which had no annotation to a biological process if strong evidence codes (other than inferred from electronic annotation, or IEA) were considered, according to the Gene Ontology Annotation (GOA) database [12]. The assay was validated by the detection of a previously known apoptosis-inducing gene, the solute carrier family 25, member 4 (*SLC25A4*). *SLC25A4* is a

mitochondrial membrane protein known to trigger apoptosis by overexpression [10]. Other than the *SLC25A4* gene, 9 further genes previously not known for their apoptotic potential were identified and 6 of these 9 were confirmed for their proapoptotic function by TUNEL assay, Nicoletti assay, and caspase inhibition. Thus, 1.8% of the screened genes induced apoptosis. Considering only strong evidence codes, the GOA database lists 18,628 gene products without annotation to a biological process [12]. Extrapolating our finding of 1.8% apoptotic genes, one could expect to identify some 330 novel proapoptotic genes by this assay, keeping in mind that extrapolation is based on small numbers. The GOA database lists 8381 genes with an annotation (non-IEA) to a biological process, 234 (2.8%) of them are proapoptotic. According to these numbers, our assay might allow for the identification of 65% of all possible proapoptotic genes.

Expression status of these genes was examined in silico in different cancer entities using the cancer microarray database Oncomine [13]. With the exception of *FLJ20551*, five of the identified proapoptotic genes were downregulated in one or more different cancer entities (Table S1) [14–19]. Thus, the functional assay presented here also allows one to pinpoint individual candidate genes with oncogenic potential.

In summary, this screening approach demonstrates that the assay is a powerful technique for the functional characterization of genes. Our method could substantially contribute to the elucidation of the function for those more than 18,000 genes for which no function has been assigned yet.

Materials and methods

Expression library

Three hundred eighty-two randomly selected human sequence-verified full-length ORFs (for a list of all genes see Table S2) from Library 970 were obtained from the RZPD. This library is a compilation of human sequence-verified full-length ORFs selected from libraries of the NIH Mammalian Gene Collection and the IMAGE Consortium. It contains clones of the *Escherichia coli* strain DH10B transformed with cDNAs unidirectionally inserted into the pCMV-Sport6 expression vector. Plasmids were isolated using the QIAprep Spin Miniprep Kit (Qiagen, Hilden, Germany).

Cell culture, reverse transfection, cell fixation

Human HEK293T (human embryonal kidney) cells (ATCC CRL-1573) were cultured in DMEM supplemented with 10% (v/v) fetal bovine serum, 100 U/ml penicillin, and 100 μg/ml streptomycin at 37°C and 5% (v/v) CO_2. Reverse transfection was based on the protocol published by Ziauddin et al. [5]. For the GDM, 0.6 μg *pEYFP* (BD Biosciences Clontech, Palo Alto, CA, USA) plasmid and 0.6 μg expression plasmid were added to 13 μl of 0.2% (w/v) gelatin solution (G-9391; Sigma–Aldrich, Munich, Germany), ensuring that the gelatin concentration was above 0.17%. The DNA–gelatin solution was arrayed in quadruplicate onto poly-L-lysine-coated Poly-Prep Slides (Sigma–Aldrich) using the Omnigrid (GeneMachines, San Carlos, CA, USA) microarrayer and SMP15B spotting pins (TeleChem International, Sunnyvale, CA, USA). Dot spacing was 1000 μm, mean spot diameter was 600 μm for all experiments. Slides were stored at room temperature in a dry atmosphere until further processing, for up to 4 weeks. Subsequently, the incubation chamber Hybri-Well (Sigma–Aldrich) with adhesive edges was attached to the spotted area and the array was incubated with the transfection reagent Effectene (Effectene Transfection Kit; Qiagen). The transfection reagent mix was prepared as follows: 150 μl EC buffer was mixed with 16 μl Enhancer and incubated for 5 min at room temperature. Twenty-five microliters of Effectene was subsequently added and the solution was distributed into the Hybri-Well and incubated for 20 min at room temperature. After the transfection reagent and the incubation chamber were removed the slide was ready for transfection.

For the LDM 0.6 μg *pEYFP* plasmid, 0.6 μg expression plasmid, and 1.5 μl Enhancer were successively added to 15 μl EC buffer containing 0.1 M sucrose. The mixture was incubated for 5 min at room temperature. Subsequently, 5 μl Effectene was added and again incubated for 10 min at room temperature. A 1× volume of 0.4% (w/v) gelatin (G-9391; Sigma–Aldrich) was mixed with the solution to complete the transfection master mix. Arrayed slides were stored as described above.

Slides were placed in QuadriPERM plates (Vivascience, Hannover, Germany), overlaid with 2.2×10^6 HEK293T cells, and cultured for 48 h in DMEM supplemented with 10% (v/v) fetal bovine serum, 100 U/ml penicillin, and 100 μg/ml streptomycin. Cells were fixed for 60 min at room temperature in 3.7% (w/v) paraformaldehyde (Merck, Darmstadt, Germany) in phosphate-buffered saline. Fixed cells were permeabilized (0.1% sodium citrate (w/v), 0.1% (v/v) Triton X-100 (Sigma–Aldrich) in phosphate-buffered saline) for 5 min, washed two times for 5 min in phosphate-buffered saline, overlaid with Vectashield mounting medium containing DAPI (Vector Laboratories, Burlingame, CA, USA), and covered with a coverslip (24 × 40 mm; R. Langenbrinck, Teningen, Germany). Slides were scanned with a GenePix 4000A microarray scanner (Axon Instruments, Union City, CA, USA) to evaluate transfection efficiency and EYFP expression. Morphologic and nuclear changes were assessed using the epifluorescence microscope Axioplan (Zeiss, Jena, Germany). Fluorescence images were acquired on the epifluorescence microscope Axioplan (Zeiss) by using the CCD camera ORCA-ER-1394 (Hamamatsu Photonics K.K., Hamamatsu City, Japan).

Standard transfection

HEK293T cells (2×10^5) in 2000 μl DMEM supplemented with 10% (v/v) fetal bovine serum, 100 U/ml penicillin, and 100 μg/ml streptomycin were seeded into six-well plates 12 h before transfection. For the TUNEL assay circular 12-mm diameter coverslips were placed into the plate before seeding. Plasmid DNA (0.5 μg) was added to 500 μl EC buffer followed by 3.2 μl Enhancer (Effectene kit; Qiagen), mixed, and incubated at room temperature. After 5 min, 10 μl Effectene was added. The mixture was incubated at room temperature for 10 min. Finally, 500 μl fresh medium was added to the ready transfection mixture. This was carefully pipetted onto the cells, and the plate was placed in an incubator at 37°C and 5% (v/v) CO_2 for 48 h. The pan-caspase inhibitor Z-VAD-fmk (Alexis Biochemicals, Grünberg, Germany) was used at 20 μM concentration and administered every 12 h due to its instability. Cells were harvested for the Nicoletti assay [20] or fixed for TUNEL assay on the coverslips as described above.

Apoptosis assays

For imaging of apoptotic nuclei, TUNEL assays were performed using the *In Situ* Cell Death Detection Kit, TMR red (Roche Diagnostics, Mannheim, Germany), according to the manufacturer's instructions.

To measure the extent of apoptosis induction by the identified proapoptotic genes, Nicoletti assays were performed. Cells from a six-well microtiter plate were harvested and washed 1× with phosphate-buffered saline. One-tenth of the amount of harvested cells was suspended in 80 μl Nicoletti buffer (0.1% (w/v) sodium citrate, pH 7.4, 0.1% (v/v) Triton X-100, 50 μg/ml propidium iodide) and incubated at 4°C in the dark. The DNA content present in the resulting nuclei was determined by FACS using a BD FACSArray Bioanalyzer System (BD Biosciences, San Jose, CA, USA). Sub-G1 cells were considered apoptotic.

Acknowledgments

We thank Armin Pscherer for helpful discussion, Sandra Steinbrink for help with FACS measurement, and Jörg Schlingemann for critical reading of the manuscript. We also thank Vinayagam Arunachalam and Nicolas Delhomme for

database analysis and Maria Shahmoradgoli for technical support. This work was supported by grants from the Bundesministerium für Bildung und Wissenschaft (Nationales Genomforschungsnetzwerk, NGFN-1, 01 GR 0101) as well as the EU MolTools program (LSHG-CT-2004-503155).

Appendix A. Supplementary data

Supplementary data associated with this article can be found in the online version at doi:10.1016/j.ygeno.2005.12.009.

References

[1] E.S. Lander, et al., Initial sequencing and analysis of the human genome, Nature 409 (2001) 860–921.
[2] C. del Val, et al., High-throughput protein analysis integrating bioinformatics and experimental assays, Nucleic Acids Res. 32 (2004) 742–748.
[3] U. Yu, S.H. Lee, Y.J. Kim, S. Kim, Bioinformatics in the post-genome era, J. Biochem. Mol. Biol. 37 (2004) 75–82.
[4] S.M. Elbashir, et al., Duplexes of 21-nucleotide RNAs mediate RNA interference in cultured mammalian cells, Nature 411 (2001) 494–498.
[5] J. Ziauddin, D.M. Sabatini, Microarrays of cells expressing defined cDNAs, Nature 411 (2001) 107–110.
[6] R. Kumar, D.S. Conklin, V. Mittal, High-throughput selection of effective RNAi probes for gene silencing, Genome Res. 13 (2003) 2333–2340.
[7] B.L. Webb, B. Diaz, G.S. Martin, F. Lai, A reporter system for reverse transfection cell arrays, J. Biomol. Screen. 8 (2003) 620–623.
[8] C. Conrad, et al., Automatic identification of subcellular phenotypes on human cell arrays, Genome Res. 14 (2004) 1130–1136.
[9] J.M. Silva, H. Mizuno, A. Brady, R. Lucito, G.J. Hannon, RNA interference microarrays: high-throughput loss-of-function genetics in mammalian cells, Proc. Natl. Acad. Sci. USA 101 (2004) 6548–6552.
[10] M.K. Bauer, A. Schubert, O. Rocks, S. Grimm, Adenine nucleotide translocase-1, a component of the permeability transition pore, can dominantly induce apoptosis, J. Cell Biol. 147 (1999) 1493–1502.
[11] J.A. Collins, C.A. Schandi, K.K. Young, J. Vesely, M.C. Willingham, Major DNA fragmentation is a late event in apoptosis, J. Histochem. Cytochem. 45 (1997) 923–934.
[12] E. Camon, et al., The Gene Ontology Annotation (GOA) project: implementation of GO in SWISS-PROT, TrEMBL, and InterPro, Genome Res. 13 (2003) 662–672.
[13] D.R. Rhodes, et al., ONCOMINE: a cancer microarray database and integrated data-mining platform, Neoplasia 6 (2004) 1–6.
[14] X. Chen, Gene expression patterns in human liver cancers, Mol. Biol. Cell 13 (2002) 1929–1939.
[15] H.F. Frierson Jr., et al., Large scale molecular analysis identifies genes with altered expression in salivary adenoid cystic carcinoma, Am. J. Pathol. 161 (2002) 1315–1323.
[16] M.E. Garber, et al., Diversity of gene expression in adenocarcinoma of the lung, Proc. Natl. Acad. Sci. USA 98 (2001) 13784–13789.
[17] C.A. Iacobuzio-Donahue, et al., Exploration of global gene expression patterns in pancreatic adenocarcinoma using cDNA microarrays, Am. J. Pathol. 162 (2003) 1151–1162.
[18] S. Ramaswamy, et al., Multiclass cancer diagnosis using tumor gene expression signatures, Proc. Natl. Acad. Sci. USA 98 (2001) 15149–15154.
[19] A. Bhattacharjee, et al., Classification of human lung carcinomas by mRNA expression profiling reveals distinct adenocarcinoma subclasses, Proc. Natl. Acad. Sci. USA 98 (2001) 13790–13795.
[20] I. Nicoletti, G. Migliorati, M.C. Pagliacci, F. Grignani, C. Riccardi, A rapid and simple method for measuring thymocyte apoptosis by propidium iodide staining and flow cytometry, J. Immunol. Methods 139 (1991) 271–279.

Web site reference

The Web site at http://www.oncomine.org provides a microarray database and integrated data-mining platform.